On the Parameterization of Geostrophic Eddies in the Ocean

JOHN C. MARSHALL

Atmospheric Physics Group, Department of Physics, Imperial College, London, England

ABSTRACT

An attempt is made to incorporate into a two-layer, zonally averaged, channel ocean model the important transfers achieved by a geostrophic eddy field, using gross parameterizations rather than resolving individual eddy events. It is shown that a representation of the eddy field as an explicit diffuser of potential vorticity can give a reasonable description of the interaction between the eddies and mean flow, provided care is taken to satisfy the attendant constraints that the zonally invariant channel geometry imposes on the eddy fields.

1. Introduction

In formulating a theory of the large-scale ocean circulation, account must be taken of both mean and turbulent transfers of quantities such as heat and vorticity.

Munk (1950) suggested that the influence of large lateral eddy transfers might be important only on the western sides of the ocean, although later observations cast doubt on the neglect of eddy vorticity transfer away from boundary regions. [See Simmons *et al.* (1977) for a review of the Mid-Ocean Dynamics Experiment (MODE).] It has now been established that mid-ocean mesoscale (geostrophic) eddies are prevalent. These eddies have a scale close to the Rossby radius of deformation (of order 50 km) and are thought to be important transferring agents of heat and vorticity. It is necessary to come to terms with a turbulent ocean full of mesoscale eddies which have a significant effect on the mean larger scale circulation. A problem for the ocean modeler is the necessity to incorporate these small space-scale eddies into a large, gyre-scale model.

Numerical models of the general circulation with sufficient horizontal resolution to include motions on the scale of the Rossby radius explicitly, within the larger scale circulation, have been constructed—the so-called eddy resolving general circulation models (EGCM). The first of these was due to Holland and Lin (1975a,b). Subsequently, others have been developed—Robinson *et al.* (1977), Semtner and Mintz (1977), Holland (1978) and McWilliams *et al.* (1978). They show the development of mesoscale eddies within the larger scale circulation. The results suggest that internal instability produces vigorous geostrophic eddies which play a crucial role in the larger scale dynamics.

If mesoscale eddies are as important in the ocean as they are in the EGCM's, one must consider the most appropriate way of incorporating them in a large-scale model.

a. The desirability of a parametric representation for the mesoscale

The mesoscale in the ocean is dynamically analogous to the synoptic scale in the atmosphere (for a review of mesoscale dynamics see Rhines, 1977). The motions are both quasi-geostrophic quasi-two-dimensional, and on the scale of the respective Rossby radii. However, there is a more serious resolution problem for the ocean modeler.

In the ocean the Rossby radius (the length scale of dynamical importance) $L\rho \sim 50$ km, compared with a horizontal extent of the domain, $L_x \sim 5000$ km. For comparison, in the atmosphere $L\rho \sim 1000$ km and $L_x \sim 10\,000$ km. So the oceanic eddies are not only smaller in absolute terms than their atmospheric counterparts, but also relative to the size of the domain. Because an ocean basin is many eddy diameters wide $(L_x/L\rho \sim 100)$ it is difficult and expensive to resolve the eddy field and, at the same time, the large-scale gyres. In order to adequately resolve the mesoscale, a resolution of 20 km or less would be required—about 100 000 grid points at each level in the vertical to resolve the North Atlantic alone (see Gill, 1971). To model the world's oceans with such a horizontal resolution is impossible at present, and probably undesirable anyway. The EGCM's reach a compromise by modeling an ocean basin which is unrealistically small. In contrast, it is far easier to resolve the synoptic scale in a global atmospheric model (in this case $L_x/L\rho \sim 10$).

A sensible goal for the ocean modeler is to develop, if possible, adequate parameterizations for the mesoscale, enabling mean quantities to be dealt with directly. It is desirable to structure ocean general circulation models in this way—explicitly resolving the three-dimensional large-scale, sluggish circulation, while parameterizing the considerably smaller scale transient eddies. Such implicit models require much less horizontal resolution and are more efficient computationally, enabling larger domains to be studied on longer time scales. The focus of attention is drawn away from an individual mesoscale event to the statistical effect of a large number of such events.

This approach has been adopted in atmospheric modeling. Models of the atmosphere with short synoptic (cyclone) scales represented by their transfer properties have been successfully constructed for use in climate research (e.g., Green, 1970; Sela and Wiin-Nielson, 1971; White and Green, 1980a,b).

It is not known at present whether an adequate mesoscale closure can be found, but in any case perhaps the greatest value of parameterized models is that they lead to greater understanding and provide a perspective from which the more complex models can be viewed.

b. The development of new parameterization schemes

In developing a parameterization scheme, one must be aware of the observational studies, using real ocean data on the scale of the process to be parameterized, and the data generated from the numerical models which aim to explicitly resolve the process. The observational and model studies that have been carried out have shown that the simple closure laws previously used are not adequate. Early theories parameterized the mesoscale in terms of an eddy-diffusivity and eddy-viscosity (Munk-type) formulation. The viscosity and diffusivity were assumed to be constant in space and time, and positive. From observations, correlations of eddy horizontal velocity components often show transfer of momentum upgradient, corresponding to a "negative viscosity" (Webster, 1961; Schmitz, 1977). In the EGCM's, the mesoscale produces eddy heat and vorticity fluxes according to the thermodynamic and hydrodynamic equations. Again, the results suggest that closures based on constant viscosity and diffusivity laws are inadequate representations of the transfer properties of the mesoscale (see, e.g., Harrison, 1978; Rhines and Holland, 1979; Holland and Rhines, 1980). A scheme based on a more detailed treatment of the mesoscale dynamics is required. An early attempt to find such a scheme was made by Welander (1973).

The development of a physically accurate closure will rely heavily on the EGCM modeling results, together with the sparse observations. Of the EGCM's, the two-layer quasi-geostrophic models provide the simplest and most useful framework in which to develop a physically realistic mesoscale parameterization.

2. The two-layer quasi-geostrophic models

The Holland (1978) and McWilliams et al. (1978, hereafter MHC) models are the simplest of the EGCM's. They are two-layer quasi-geostrophic, β-plane models, driven by a sinusoidal wind stress and have minimal explicit diffusion. The stratification and layer thicknesses are chosen to give realistic values of the Rossby radius. The horizontal resolution is chosen to adequately resolve motions on this scale. The Holland (1978) closed-basin model can be regarded as an extension of the Veronis (1966) one-layer, nonlinear model, to include high resolution and stratification; that of MHC, on the other hand, considers a partially blocked channel as an approximation of the Antarctic Circumpolar Current. It has many features in common with atmospheric flows.

The model equations can be written [for a derivation see Pedlosky (1964) or McWilliams (1977)]

$$\frac{D_1}{Dt_h} (\xi_1 + f) + \frac{f_0}{H_1} W_2 = \frac{\mathbf{k} \cdot \mathrm{curl}\tau_1}{H_1} - \Delta_1, \quad (1a)$$

$$\frac{D_3}{Dt_h} (\xi_3 + f) - \frac{f_0}{H_3} W_2 = - \frac{\mathbf{k} \cdot \mathrm{curl}\tau_3}{H_3} - \Delta_3, \quad (1b)$$

$$\frac{D_2}{Dt_h} (\psi_1 - \psi_3) + \frac{g'}{f_0} W_2 = 0, \quad (2)$$

where the upper layer is denoted by a subscript 1, the lower layer by a subscript 3, the interface by a subscript 2, ψ_i is the streamfunction, $\xi_i = \nabla^2 \psi_i$ is the relative vorticity, ρ_1 and ρ_3 are the layer densities, $g' = g(\rho_3 - \rho_1)/\rho_3$ is the reduced gravity, H_i are the layer thicknesses, $\mathbf{k} \cdot \mathrm{curl}\tau_i$ is the vertical component of the external stress, W_2 is the vertical velocity at the interface, $f = f_0 + \beta_0 y$ (with f_0 and β_0 constants) is the Coriolis parameter, $D_i/Dt_h = \partial/\partial t + J(\psi_i, \ )$ is the substantial derivative, and Δ_i is the explicit diffusion.

Eq. (1) expresses the non-conservation of absolute vorticity due to the effect of vortex stretching and the presence of vorticity sources and sinks. Eq. (2) is a continuity equation predicting the deviation of the height of the interface from its equilibrium position, $h_I = f_0(\psi_3 - \psi_1)/g'$. It can be looked on as a thermodynamic equation for the temperature at the interface, which is proportional to $(\psi_1 - \psi_3)$.

Eliminating W_2 from (1), using (2), leads to the potential vorticity equations

$$\frac{D_1}{Dt_h}(q_1) = \frac{\mathbf{k}\cdot\mathrm{curl}\boldsymbol{\tau}_1}{H_1} - \Delta_1, \qquad (3a)$$

$$\frac{D_3}{Dt_h}(q_3) = -\frac{\mathbf{k}\cdot\mathrm{curl}\boldsymbol{\tau}_3}{H_3} - \Delta_3, \qquad (3b)$$

where

$$q_1 = \xi_1 + f - \frac{f_0^2}{g'H_1}(\psi_1 - \psi_3),$$

$$q_3 = \xi_3 + f + \frac{f_0^2}{g'H_3}(\psi_1 - \psi_3).$$

Eq. (3) expresses the conservation of the potential vorticities, q_1 and q_3 except for changes caused by external stress and molecular diffusion.

a. The averaged equations

The philosophy adopted in Holland (1978) and MHC is to integrate the set forward in time from a prescribed initial state and to examine the final statistically steady state in which the eddy and mean fields are in equilibrium. Once in the final equilibrium state, the fields are divided into a mean part (denoted by an overbar, representing some averaging procedure) and a fluctuating or eddy part (denoted by a prime), i.e.,

$$\psi_i = \overline{\psi_i} + \psi_i' \quad \text{and} \quad \overline{\psi_i'} = 0.$$

Eddy transfer is introduced by averaging the advection terms. Substituting into (1) and (2) and averaging, gives

$$\frac{\bar{D}_1}{Dt_h}(\bar{\xi}_1 + f) + \boldsymbol{\nabla}_h\cdot\overline{(\mathbf{v}_1'\xi_1')} + \frac{f_0}{H_1}\bar{W}_2$$

$$= \frac{\mathbf{k}\cdot\mathrm{curl}\bar{\boldsymbol{\tau}}_1}{H_1} - \bar{\Delta}_1, \qquad (4a)$$

$$\frac{\bar{D}_3}{Dt_h}(\bar{\xi}_3 + f) + \boldsymbol{\nabla}_h\cdot\overline{(\mathbf{v}_3'\xi_3')} - \frac{f_0}{H_3}\bar{W}_2$$

$$= -\frac{\mathbf{k}\cdot\mathrm{curl}\bar{\boldsymbol{\tau}}_3}{H_3} - \bar{\Delta}_3, \qquad (4b)$$

$$\frac{\bar{D}_2}{Dt_h}(\bar{\psi}_1 - \bar{\psi}_3) + \boldsymbol{\nabla}_h\cdot\overline{(\mathbf{v}_2'(\psi_1' - \psi_3'))}$$

$$+ \frac{g'}{f_0}\bar{W}_2 = 0, \qquad (5)$$

or, in terms of potential vorticity

$$\frac{\bar{D}_1}{Dt_h}(\bar{q}_1) + \boldsymbol{\nabla}_h\cdot\overline{(\mathbf{v}_1'q_1')} = \frac{\mathbf{k}\cdot\mathrm{curl}\bar{\boldsymbol{\tau}}_1}{H_1} - \bar{\Delta}_1, \qquad (6a)$$

$$\frac{\bar{D}_3}{Dt_h}(\bar{q}_3) + \boldsymbol{\nabla}_h\cdot\overline{(\mathbf{v}_3'q_3')} = -\frac{\mathbf{k}\cdot\mathrm{curl}\bar{\boldsymbol{\tau}}_3}{H_3} - \bar{\Delta}_3. \qquad (6b)$$

The averaged potential vorticity equations may be derived directly from (3) or from the averaged vorticity and thermodynamic equations, (4) and (5), with use of the following relationships between the eddy fluxes of relative vorticity, potential vorticity and heat:

$$\boldsymbol{\nabla}_h\cdot\overline{(\mathbf{v}_1'\xi_1')} = \boldsymbol{\nabla}_h\cdot\overline{(\mathbf{v}_1'q_1')}$$

$$+ \frac{f_0^2}{g'H_1}\boldsymbol{\nabla}_h\cdot\overline{[\mathbf{v}_2'(\psi_1' - \psi_3')]}, \qquad (7a)$$

$$\boldsymbol{\nabla}_h\cdot\overline{(\mathbf{v}_3'\xi_3')} = \boldsymbol{\nabla}_h\cdot\overline{(\mathbf{v}_3'q_3')}$$

$$- \frac{f_0^2}{g'H_3}\boldsymbol{\nabla}_h\cdot\overline{[\mathbf{v}_2'(\psi_1' - \psi_3')]}. \qquad (7b)$$

In a parameterized model, instead of integrating (1) and (2) forward (requiring high resolution in space and time) and then averaging, mean quantities are dealt with directly through (4) and (5) (requiring lower resolution in space and time). In such a model a separation between eddy and mean fields is made from the start, and the two interact through the eddy flux divergence terms. In the explicit models the eddy transfers are achieved by resolved eddies, but in the implicit model the transfers must be represented in terms of the mean fields by a closure hypothesis.

b. Geometrical effects

As a consequence of the different geometry at the large-scale, the basin model of Holland (1978) and the channel model of MHC exhibit quite different dynamics.

In the gyre model the flow is more greatly curved due to the presence of meridional walls which obstruct zonal flow, and impose zonal gradients. The classical Sverdrup balance plays an important role, although severely distorted by eddy transfer. In the channel model the flow is more zonal and driven more directly by the wind.

Of particular importance, in the context of the closure problem, is the effect of the large-scale geometry on the instability processes. In the channel model, since the geometry is zonally invariant, eddies do not develop at preferred locations along the flow. If the flow is unstable it is unstable at all longitudes, and the effect of the eddies is to transfer potential vorticity down the local gradient. The gyre model is more complicated. Here the presence of meridional walls impose such large zonal gradients that the regions of eddy generation are more localized, advective effects greater, and the regions of eddy decay more extensive. Much of the basin is populated by decaying eddies, which cannot be expected to transfer potential vorticity systematically down the local gradient.

The contrasts between the channel models, with

simple periodic geometry at the large-scale and the gyre models, zonally blocked by meridional walls, are more fully developed in Holland and Rhines (1980). They suggest that the zonally blocked flow regimes will present a more complicated parameterization problem than the zonally open ones, although in channel flow a diffusive parameterization for potential vorticity may be appropriate. Accordingly, as a first candidate for modeling we choose flow in periodic channel geometry. It is in this flow regime that a diffusive parameterization for potential vorticity is most likely to give an adequate representation of the interaction between the mesoscale and the large-scale.

3. A zonally averaged channel model

Here a two-layer channel, zonally averaged ocean model is fomulated. The mathematical model does not attempt to approximate a real ocean regime. The same problem is tackled as in the flat-bottomed open-channel simulations of MHC, except that here the time and zonally averaged quantities are dealt with directly, using a low resolution and gross representations for the eddy field.

The model domain is a zonal channel with a repeat length L_x. The channel walls lie along latitude circles, a distance L apart. The bottom is flat and there are no meridional walls. The momentum source for the mean currents is a surface wind stress, and the momentum sink is through bottom friction. It is assumed that the necessary fluxes needed to maintain the mean currents can be accomplished by a quasi-geostrophic eddy field. The eddy field is represented through its transfer properties. There is no small-scale explicit lateral diffusion.

With thermal forcing and appropriate choice of constants, the model could easily be interpreted as a two-level atmospheric model (as MHC point out, the two-layer and two-level equations are identical in the quasi-geostrophic approximation). The close link with the zonally averaged parameterized atmospheric models is then apparent. The particular formulation used here is closest to that of Sela and Wiin-Nielson (1971).

a. The zonally averaged equations

Integrating the problem with $\bar{q}$ as a dependent variable, using the zonally averaged Eq. (6), is attractive since potential vorticity is a fundamental constraint on the fluid motion. Such an approach is a considerable simplification from the closure point of view. For the purposes of the time integration, it is not necessary to parameterize the eddy fluxes of heat and vorticity separately, but only the flux of potential vorticity. Further potential vorticity is con-

served in advection by the horizontal component of the flow (unlike temperature and vorticity). Its close conservation on the time scale of the transfer suggests a tendency for the eddies to transfer potential vorticity down the mean gradient. For a discussion of the applicability of diffusive parameterizations in closed and channel ocean models see Holland and Rhines (1980).

Choosing the overbar in (6) to represent a time and zonal average, the terms representing advection by the mean disappear and the model equations become

$$\frac{\partial \bar{q}_1}{\partial t} = - \frac{\partial}{\partial y} \overline{(v_1' q_1')} - \frac{1}{H_1} \frac{\partial \bar{\tau}_1}{\partial y} , \qquad (8a)$$

$$\frac{\partial \bar{q}_3}{\partial t} = - \frac{\partial}{\partial y} \overline{(v_3' q_3')} + \frac{1}{H_3} \frac{\partial \bar{\tau}_3}{\partial y} , \qquad (8b)$$

where

$$\overline{()} = \frac{1}{T L_x} \int_t^{t+T} \int_0^{L_x} () dx dt$$

and L_x is the repeat length of the channel, long compared with an eddy length scale, and T is the averaging period, long compared with an eddy lifetime.

The Sverdrup balance, which dominates the dynamics of the ocean gyres, plays no role here. A mean geostrophic meridional velocity cannot be supported by a zonal pressure gradient (by piling up water between meridional walls). In the upper layer, the wind-stress curl is balanced, not by the mean advection of potential vorticity (the β-term), but by an eddy flux divergence. To this extent eddy transfer is far more crucial in the present geometry than for the closed ocean-basin regime.

In the MHC simulation, the eddies are found to transfer potential vorticity down the mean gradient almost everywhere, suggesting that the transfer may be modeled as a diffusive process. Accordingly, the eddy flux of potential vorticity is assumed to be related to the mean q field through the diffusive transfer equations

$$\overline{v_i' q_i'} = -K_i \frac{\partial \bar{q}_i}{\partial y} \quad i = 1 \text{ and } 3, \qquad (9)$$

where the K_i's are eddy transfer coefficients which, in general, can be functions of space and time (see Green, 1970). Assuming a knowledge of the transfer coefficients, Eq. (9) provides a closure for the eddy potential vorticity flux.

b. General considerations

Having adopted a transfer theory, one is then faced with the problem of how to specify the magnitude and spatial form of the transfer coefficients. In the ocean little is known about the variation of the K's in the horizontal and vertical. The form and

magnitude will depend crucially on the intensity, length and time scales and the vertical structure of the eddies. Results can be expected to be sensitive to the particular choice made. Further, one must be careful in the choice, for it is not possible to freely diffuse vorticity around without taking into account basic constraints on the eddy field (see White, 1977). In particular, it is important that the parameterized scales should not lead to sources and sinks of momentum not generated by the explicitly resolved eddies. Thomson and Stewart (1977) have highlighted this difficulty in the context of the work of Welander (1973).

The choice of the form of the transfer coefficients should be guided by a knowledge of the structure of the transferring agent. If it is hypothesized that in fully turbulent flow the eddies are those that would have amplified from an instability of the mean flow, then a linear instability analysis can give clues about the structure. Green (1970) made use of the idea that, since the shape of the eddies does not unrecognizably change as they reach finite amplitude, much of the essential structure of the atmospheric cyclones and anticyclones can be ascertained from baroclinic instability analyses of the zonal flow. One must be apprehensive, however, about the appropriateness of perturbation arguments for the transfer properties of fully developed, nonlinear eddies. Hoskins and Simmons (1978), for example, show how radically different linear and nonlinear results can be regarding the Reynold's stresses. In any case, the interest is not in the transfers achieved by one eddy, but the statistical effect of many eddies.

In an attempt to develop an approach that does not rely so heavily on linear theory, and at the same time to ensure that the parameterized scales do not lead to any spurious sources and sinks of momentum, White and Green (1980a) suggested that the gross forms of the K's should be specified drawing on our knowledge of the dynamics of the turbulence, with the finer details determined by adjusting the forms until a vorticity flux constraint is satisfied. This approach is adopted here. We will assume that the eddies are generated by a baroclinic instability of the mean flow (as in the MHC simulations), plausibly specify the form of the transfer coefficients in the light of this mechanism, and then, to give more detail, exploit the vorticity constraint appropriate to the channel geometry.

c. A constraint on the depth integrated meridional potential vorticity flux

In the case of an eddy defined as a deviation from a time and zonal average, the eddy fluxes of heat, vorticity and potential vorticity are related as follows:

$$\overline{v_1'\xi_1'} = -\frac{\partial}{\partial y}(\overline{u_1'v_1'})$$

$$= \overline{v_1'q_1'} + \frac{f_0^2}{g'H_1}\overline{v_2'(\psi_1' - \psi_3')}, \quad (10a)$$

$$\overline{v_3'\xi_3'} = -\frac{\partial}{\partial y}(\overline{u_3'v_3'})$$

$$= \overline{v_3'q_3'} - \frac{f_0^2}{g'H_3}\overline{v_2'(\psi_1' - \psi_3')}. \quad (10b)$$

Eq. (10) may be derived from (7) by integrating with respect to y. The constants of integration are zero, for the eddy fluxes must go to zero at the walls.

Multiplying (10a) by H_1, (10b) by H_3 and adding, the heat flux term vanishes, leaving a relation between the depth-integrated fluxes of potential vorticity and vorticity:

$$-H_1\frac{\partial}{\partial y}(\overline{u_1'v_1'}) - H_3\frac{\partial}{\partial y}(\overline{u_3'v_3'})$$

$$= H_1\overline{v_1'q_1'} + H_3\overline{v_3'q_3'}. \quad (11)$$

Integrating with respect to y from one channel wall to the other (on which $\overline{u'v'} = 0$), the vorticity flux integrates out to zero giving

$$\int_0^L H_1\overline{v_1'q_1'} + H_3\overline{v_3'q_3'}\,dy = 0. \quad (12)$$

Dynamically, (12) ensures the quasi-geostrophic eddy field cannot provide a net acceleration of the flow, but merely acts to redistribute momentum

$$\frac{\partial}{\partial t}\int_0^L H_1\bar{u}_1 + H_3\bar{u}_3 dy = 0$$

in the absence of sources and sinks. Substituting in (12) for the potential vorticity fluxes, using the transfer equations (9), enforces a relationship between the transfer coefficients.

$$\int_0^L H_1K_1\frac{\partial\bar{q}_1}{\partial y} + H_3K_3\frac{\partial\bar{q}_3}{\partial y}\,dy = 0. \quad (13)$$

For the special case of an infinitesimal wave amplifying on a zonal flow, (9) are exact relations with the K's given by (see Green, 1970; Held, 1975)

$$K_i = \frac{1}{2}kC_I\frac{|\psi_i|^2}{|\bar{u}_i - C|^2}e^{2kC_It}, \quad i = 1 \text{ and } 3, \quad (14)$$

where ψ_i is the perturbation streamfunction from a mean zonal flow $\bar{u}_i$, k is the wavenumber and C_I is the imaginary part of the complex wave speed C. In particular the K's are positive, and so (13) becomes a statement of the Pedlosky (1964) necessary condition for instability that $\partial\bar{q}/\partial y$ must take on both signs somewhere in the flow. In the more

general finite-amplitude case, if the K's are positive, then $\partial \bar{q}/\partial y$ must again change sign. In the MHC simulations the K's are positive almost everywhere and the potential vorticity gradients have opposite signs in the two layers, rather than different signs in the same layer at different latitudes.

d. Specification of the K's

Here (13) is exploited to give information about the variation of the K's in the vertical. The horizontal variation of the K's is prescribed and (13) used to relate K_1 and K_3.

The K's are written in the form

$$K_i = k_i Y_i(y), \quad i = 1 \text{ and } 3, \tag{15}$$

where $Y_i(y)$ gives the (normalized) meridional variation of the K's and k_i gives the magnitude.

First, we consider the specification of the meridional variation. For motions of infinitesimal amplitude the K's [given by (14)] are positive and depend on the distribution of the eddy kinetic energy, proportional to $k^2 |\hat{\psi}_i|^2$, but also on the phase speed of the disturbance relative to the mean flow speed, $|\bar{u}_i - C|^2$. In baroclinically unstable channel flow the eddy kinetic energy decreases sharply away from the region of large temperature gradient in mid-channel (see, e.g., the plot of $\overline{\psi_1'^2}$, Fig. 4, in MHC) suggesting that the K profile should be peaked sharply in the region of maximum baroclinity. The K's, however, also will be large on the flanks of the jet, where $|\bar{u}_i - C|^2$ is small, for here parcels of fluid move only slowly relative to the disturbance and so suffer large lateral displacements. This tendency will broaden the meridional profile obtained from a consideration of the eddy kinetic energy distribution alone. The net effect is likely to make the K's large in midchannel, where eddy parcels readily disperse laterally, and smaller at the extremities of the jet, where dispersion is inhibited by the channel walls. The K's will be zero at the wall. These gross features are likely to be true even of the K's appropriate to fully turbulent flow. Although, in general, the K's can be expected to be non-separable (see White and Green, 1980a), in view of the lack of detailed knowledge, we prefer to avoid the complication of specifying two different functional forms (one for each layer). Instead, as a crude representation of the essential features of the horizontal variation, we choose the separable form

$$Y_i(y) = Y(y) = \frac{|\bar{u}_1 - \bar{u}_3|}{|\bar{u}_1 - \bar{u}_3|_{max}}, \quad i = 1 \text{ and } 3. \tag{16}$$

The specification is attractive for it models the concentration of baroclinic activity in the regions of large temperature gradients, allows some feedback between the local flow field and the K's, ensures

the K's are positive and, anticipating the application of the no-slip boundary condition, brings the K's to zero at the walls.

Having specified $Y(y)$, Eq. (13) is now used to give the relative magnitude of the K's. Substituting for K_1 and K_3 in (13), using (15) and (16), gives

$$\frac{k_3}{k_1} = \frac{H_1}{H_3} \frac{\left(\overline{\dfrac{\partial \bar{q}_1}{\partial y}}^y \right)}{\left(\overline{\dfrac{\partial \bar{q}_3}{\partial y}}^y \right)}, \tag{17}$$

where

$$\overline{\frac{\partial \bar{q}_i}{\partial y}}^y = \frac{\displaystyle\int_0^L \frac{\partial \bar{q}_i}{\partial y} Y dy}{\displaystyle\int_0^L Y dy}, \quad i = 1 \text{ and } 3$$

is a weighted-average potential vorticity gradient over the channel, with the weighting function given by the horizontal variation of the K's.

The physical interpretation of (17) is clearer if flow is considered in which the relative vorticity gradient, $\partial \bar{\xi}_i/\partial y$ is negligible compared with the planetary vorticity gradient β_0. Then (17) can be written in the form

$$\frac{k_3}{k_1} = \frac{1 + \gamma_1}{1 - \gamma_3},$$

where

$$\gamma_1 = \frac{H_1}{\bar{h}_0^y}, \quad \gamma_3 = \frac{H_3}{\bar{h}_0^y},$$

and $\bar{h}_0 = (f_0^2/g'\beta_0)(\bar{u}_1 - \bar{u}_3)$ is the depth scale of the baroclinic disturbance.

Eastward flows ($\gamma_1, \gamma_3 > 0$) will be unstable provided that $\gamma_3 < 1$—unstable waves extend up into the top layer, with $k_3/k_1 > 1$. Westward flows ($\gamma_1, \gamma_3 < 0$) will be unstable provided that $|\gamma_1| < 1$ —unstable waves extend down into the lower layer, with $0 < k_3/k_1 < 1$. If $H_1 < H_3$ it is easier for a westward flow to reverse the potential vorticity gradients in the thin upper layer than it is for eastward flows, and so (17) can be satisfied more readily. The link with Pedlosky's necessary condition for instability is clear.

It is through (17) that the closure hypothesis reflects the asymmetry in the vertical structure of the eddies, and the different stability characteristics of eastward and westward flows. The transfer coefficients are ascribed positive values (the flow is supposed unstable) provided the ratio k_3/k_1, given by (17) is positive. If (17) is negative, then k_1 and k_3 are held at zero (the flow is supposed stable).

To complete the closure the magnitude of the K's is required. Observations and numerical models indicate (see, e.g., Rhines and Holland, 1979)

that a diffusivity of $\sim 10^2$ m^2 s^{-1} is appropriate to quiet ocean regions, and it may rise to a value as high as 10^4 m^2 s^{-1} in vigorously unstable regions. Here the problem of relating the magnitude of the K's to bulk mean flow parameters is not tackled. Rather, the magnitude is prescribed.

With k_1 (or k_3) fixed, Eqs. (9), (15), (16) and (17) provide a closure for the eddy potential vorticity flux. With suitable initial and boundary conditions, (8) can now be integrated forward in time to predict the new $\bar{q}_1$ and $\bar{q}_3$. The results of the integration of the equations represents a practical measure of the appropriateness of the closure as a representation of the interaction between the eddies and the mean flow.

e. The closed set of equations

In (8) the following forms for the stress are adopted: a sinusoidal surface wind stress

$$\bar{\tau}_1 = \tau_0 \sin\left(\frac{\pi y}{L}\right) , \qquad (18a)$$

giving a maximum eastward stress in midchannel and zero at the walls, and a linear bottom-stress law

$$\bar{\tau}_3 = H_3 \epsilon \bar{u}_3 . \qquad (18b)$$

The dimensional variables in (8) are replaced by nondimensional variables defined by

$$\left. \begin{array}{ll} \bar{q}_i = \beta_0 L \bar{q}_i{}^* , & y = L y^* , \quad \bar{u}_i = u_C \bar{u}_i{}^* \\[2mm] k_i = u_C L\rho k_i{}^* , & \epsilon = \beta_0 L \epsilon^* , \quad t = \left(\dfrac{L\rho}{u_C}\right) t^* \end{array} \right\} ,$$

where u_C is a typical channel velocity and $L\rho$ is the Rossby radius of deformation.

Substituting for the eddy flux terms (with the closure (9), (15), (16) and (17)) the zonally averaged model takes the form of two coupled diffusion equations with non-constant coefficients, and may be written (nondimensionalized) as

$$\frac{\partial \bar{q}_1{}^*}{\partial t^*} = \gamma^2 k_1{}^* \frac{\partial}{\partial y^*}\left(Y^* \frac{\partial \bar{q}_1{}^*}{\partial y^*}\right)$$
$$- \gamma\left(\frac{u_S}{u_C}\right)\cos\pi y^* , \qquad (19a)$$

$$\frac{\partial \bar{q}_3{}^*}{\partial t^*} = \gamma^2 k_3{}^* \frac{\partial}{\partial y^*}\left(Y^* \frac{\partial \bar{q}_3{}^*}{\partial y^*}\right)$$
$$+ \gamma\epsilon^* \frac{\partial \bar{u}_3{}^*}{\partial y^*} , \qquad (19b)$$

where

$$Y^* = \frac{\left|\bar{u}_1{}^* - \bar{u}_3{}^*\right|}{\left|\bar{u}_1{}^* - \bar{u}_3{}^*\right|_{\max}} , \qquad (20)$$

$$\frac{k_3{}^*}{k_1{}^*} = -\frac{\delta_1}{\delta_3} \frac{\overline{\dfrac{\partial \bar{q}_1{}^*}{\partial y^*}}^{y^*}}{\overline{\dfrac{\partial \bar{q}_3{}^*}{\partial y^*}}^{y^*}} , \qquad (21)$$

$$\left. \begin{array}{l} u_C = \dfrac{g'\beta_0 H}{f_0{}^2} , \quad u_S = \dfrac{\pi\tau_0}{H_1\beta_0 L} , \\[4mm] \gamma = \dfrac{L\rho}{L} \\[4mm] \delta_1 = \dfrac{H_1}{H} , \quad \delta_3 = \dfrac{H_3}{H} , \\[4mm] L\rho = \left(\dfrac{g'H_1 H_3}{f_0{}^2 H}\right)^{1/2} \end{array} \right\} . \qquad (22)$$

In (22) u_C is chosen in anticipation that vertical shears will build up sufficiently to balance the β_0 term in $\partial\bar{q}/\partial y$. With this velocity nondimensionalization, the layer potential vorticity gradients are

$$\frac{\partial \bar{q}_1{}^*}{\partial y^*} = \bar{\beta}_1{}^* + \frac{1}{\delta_1}(\bar{u}_1{}^* - \bar{u}_3{}^*) , \qquad (23a)$$

$$\frac{\partial \bar{q}_3{}^*}{\partial y^*} = \bar{\beta}_3{}^* - \frac{1}{\delta_3}(\bar{u}_1{}^* - \bar{u}_3{}^*) , \qquad (23b)$$

where

$$\bar{\beta}_i{}^* = 1 - \frac{\gamma^2}{\delta_1 \delta_3} \frac{\partial^2 \bar{u}_i{}^*}{\partial y^{*2}} , \quad i = 1 \text{ and } 3 \qquad (24)$$

is the absolute vorticity gradient.

f. Method of solution

Starting from a known initial state (19) may be stepped forward numerically to give the new values of $\bar{q}_1{}^*$, and $\bar{q}_3{}^*$. To integrate further, it is necessary to compute the updated velocity field from the potential vorticity field. This is done by solving the following equations, derivable from (23) by addition and subtraction:

$$\gamma^2 \frac{\partial^2 \bar{u}_D{}^*}{\partial y^{*2}} - \bar{u}_D{}^* = -\delta_1 \delta_3 \frac{\partial}{\partial y^*}(\bar{q}_1{}^* - \bar{q}_3{}^*) , \qquad (25)$$

$$\gamma^2 \frac{\partial^2 \bar{u}_I{}^*}{\partial y^{*2}} = \delta_1 \delta_3\left[1 - \frac{\partial}{\partial y^*}(\delta_1 \bar{q}_1{}^* + \delta_3 \bar{q}_3{}^*)\right] , \qquad (26)$$

where

$$\bar{u}_D{}^* = \bar{u}_1{}^* - \bar{u}_3{}^*$$

is the velocity difference and

$$\bar{u}_I{}^* = \delta_1 \bar{u}_1{}^* + \delta_3 \bar{u}_3{}^*$$

is the depth integrated velocity.

Appropriate boundary conditions for the solution of (25) and (26) may be ascertained by considering the zonally averaged zonal momentum equation. In the absence of explicit small-scale diffusion, it can be written as

$$\frac{\partial}{\partial t}\, \bar{u}_i = f\bar{v}_i + \overline{v_i'\xi_i'} + \frac{\bar{\tau}_i}{H_i}, \quad i = 1 \text{ and } 3 \quad (27)$$

(the zonally averaged Coriolis torque, $f\bar{v}_i$, contains only the ageostrophic part of the horizontal flow).

From (27), provided that there is no stress at the walls ($\bar{\tau}_i = 0$), the flow will not accelerate. Thus, if $\bar{u}_1^*$ and $\bar{u}_3^*$ are zero initially, they will remain zero. Accordingly, the no-slip boundary condition is applied

$$\bar{u}_1^* = \bar{u}_3^* = 0, \quad \text{at} \quad y^* = 0, 1. \quad (28)$$

It is a consistent condition in view of the choice of surface stress, (18a) and the bottom-friction parameterization adopted, (18b). The appropriate boundary conditions for (25) and (26) therefore are

$$\bar{u}_I^* = \bar{u}_D^* = 0, \quad \text{at} \quad y^* = 0, 1.$$

For the time integration of (19), it is not necessary to impose a condition on $\bar{q}^*$ or $\partial\bar{q}^*/\partial y^*$, but only on $K^*\partial\bar{q}^*/\partial y^*$. Eq. (28) is sufficient for it ensures that [from Eq. (20)] the K's are zero at the walls—$K^*\partial\bar{q}^*/\partial y^*$ zero and no eddy potential vorticity flux through the solid walls.

4. Results

a. Numerical constants

The following constants are chosen to correspond to those of the MHC simulations:

$$H_1 = 10^3 \text{ m}, \quad H_3 = 4 \times 10^3 \text{ m}$$

$$\beta_0 = 1.4 \times 10^{-11} \text{ m}^{-1} \text{ s}^{-1}$$

$$L = 10^6 \text{ m}, \quad g' = 2 \times 10^{-2} \text{ m s}^{-2}$$

$$\tau_0 = 10^{-4} \text{ m}^2 \text{ s}^{-2}$$

$$f_0 = 10^{-4} \text{ s}^{-1}, \quad \epsilon = 10^{-7} \text{ s}^{-1}$$

giving $\quad\quad\quad\quad\quad\quad\quad\quad\quad\quad\quad\quad$ (29)

$$L_\rho = 4 \times 10^4 \text{ m}, \quad u_C = 1.4 \times 10^{-1} \text{ m s}^{-1},$$

$$u_S = 2.2 \times 10^{-2} \text{ m s}^{-1}$$

$$\epsilon^* = 7.1 \times 10^{-3}, \quad \gamma = 4 \times 10^{-2},$$

$$\delta_1 = 2 \times 10^{-1}, \quad \delta_3 = 8 \times 10^{-1}$$

For the above parameters a $\bar{u}^*$ of 1 corresponds to a $\bar{u}$ of 0.14 m s^{-1} and a Δt^* of 1 corresponds to a Δt of about three days.

The magnitude of k_1^* is fixed and held constant: $Y^*(y)$, however, allows a meridional variation of the transfer coefficient. MHC estimate from their

channel simulation an upper layer coefficient of about 10^3 m^2 s^{-1}. A dimensional k_1 of 10^3 m^2 s^{-1} corresponds to a nondimensional k_1^* of 0.18 given (29).

The grid spacing chosen is $\Delta y = 50$ km, giving a coarse resolution compared with the Rossby radius of 40 km ($\Delta y^*/\gamma = 1.25$).

For the (explicit) numerical time integration scheme adopted, there is a limitation on the time step. The problem is complicated by the fact that the diffusive time scales in the upper and lower layers are not the same. The time step must be less than the upper/lower grid-length diffusive time scale (whichever is the shorter)

$$\Delta t^* \leqslant \frac{1}{k^*}\left(\frac{\Delta y^*}{\gamma}\right)^2.$$

For a $\Delta y^*/\gamma$ of 1 and a k^* of 0.1, $\Delta t^* \leqslant 10$, whereas for a k^* of 1.0, Δt^* can be only $\leqslant 1$, a small increment when compared with the time scale of the mean flow, $(\gamma\epsilon^*)^{-1} \approx 4000$. In the early stages of the time integration, however, the diffusive limitation does not apply because the Pedlosky-type condition (17) is negative and so the K's are held at zero. This not only prevents numerical instability through attempting to integrate the diffusion equation backward, but also enables a much longer time step to be taken. Only in the later, diffusive stages of the time integration is the small time step required. The following results are the steady-state solutions to (19) for the case $k_1^* = 0.18$ and the constants (29).

b. Zonal velocity and potential vorticity fields

The mean velocity (Fig. 1a) consists of two zonal jets. There are no return flows. The upper and lower layer jets are similar in meridional structure, but differ in strength. The upper layer is stronger than the lower, although the zonal mass flux of the lower is greater.

The terms in the layer potential vorticity gradients, (23) and (24) are plotted in Figs. 1b and 1c. The mean layer potential vorticity gradients have opposite signs at all latitudes—the upper layer gradients are large and positive, the lower layer gradients small and negative. The background reference potential vorticity gradient β_0 is severely distorted by the interface tilt. In the upper layer the interface tilt is the dominant contribution to $\partial\bar{q}_1^*/\partial y^*$, intensifying it in midchannel to a value many times β_0. In the lower layer the absolute vorticity gradient and tilt terms are comparable. $\partial\bar{q}_3^*/\partial y^*$ is a small negative residual between these two terms. In both layers the relative vorticity gradient contributes importantly to the absolute vorticity gradient, particularly in the lower layer. In midchannel $\partial\bar{\xi}_i^*/\partial y^*$ reinforces β_0 and opposes it at the extremities. Nowhere is the curvature of the flow profile large enough to over-

power β_0, and so reverse the absolute vorticity gradient.

c. Balances in the steady-state momentum equations

The steady-state layer momentum equations may be written

$$\bar{\tau}_1 + H_1\overline{v_1'q_1'} = 0, \tag{30a}$$

$$-\bar{\tau}_3 + H_3\overline{v_3'q_3'} = 0. \tag{30b}$$

Eq. (30) can be derived from (8) by integrating with respect to y, and noting that $\bar{\tau}_1$ and $\bar{\tau}_3$ are zero at the walls.

The eddy potential vorticity fluxes are shown in Fig. 1d. In the upper layer the imposed surface wind stress is balanced by a southward eddy flux of potential vorticity. In the lower layer the bottom stress is balanced by a northward eddy flux of potential vorticity. At each latitude the eddy fluxes are almost equal in magnitude, but of opposite sign.

Adding (30a) and (30b) together and using (11) gives the vertically integrated steady-state momentum equation

$$\bar{\tau}_1 - \bar{\tau}_3 + H_1\overline{v_1'\xi_1'} + H_3\overline{v_3'\xi_3'} = 0. \tag{31}$$

Eq. (31) expresses the well-known result that the depth integrated momentum equation only feels the depth integrated flux of relative vorticity (Green, 1970).

The vertically integrated eddy potential vorticity fluxes also are plotted in Fig. 1d. Locally the surface and bottom stresses are almost, but not quite, in balance. At any latitude the difference between the surface and bottom stresses is balanced by the height integrated flux of relative vorticity (≡ height integrated flux of potential vorticity). The parameterized scales are transferring momentum into the current.

Integrating across the channel gives the integral balance

$$\int_0^L \bar{\tau}_1 dy = \int_0^L \bar{\tau}_3 dy. \tag{32}$$

Eq. (32) shows how angular momentum in the atmosphere is transferred to the solid earth via the ocean. Knowledge of this integral balance is automatically incorporated into the parameterization scheme through the constraint (17).

The upper layer transfer coefficient has a value (prescribed) of 10^3 m^2 s^{-1}. In the steady state the ratio of the transfer coefficients is

$$\frac{k_3}{k_1} = 8.6$$

giving a lower layer transfer coefficient of 8.6×10^3 m^2 s^{-1}. The particle diffusivity becomes large in the lower layer to compensate for the small negative potential vorticity gradient there. The eddy parcels
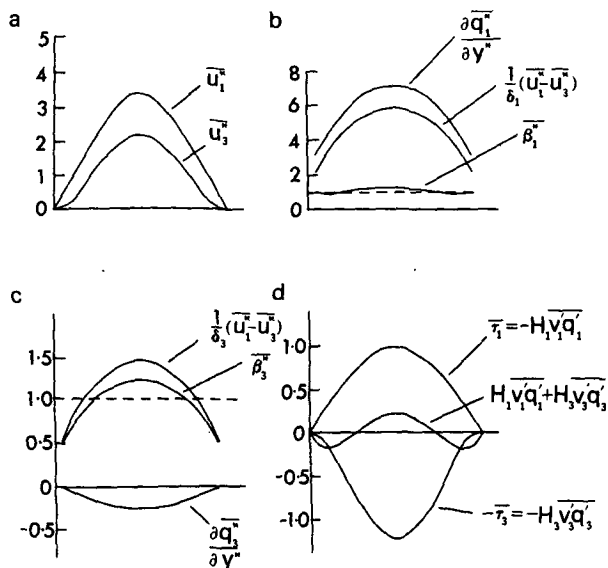

FIG. 1. Meridional profiles for the steady-state solution $k_1^* = 0.18$: (a) Nondimensionalized zonal velocity; (b) nondimensionalized upper layer potential vorticity gradient [Eq. (23a)]; (c) nondimensionalized lower layer potential vorticity gradient [Eq. (23b)]; and (d) depth-integrated momentum budget [Eq. (31)] in units of 10^{-4} m^2 s^{-2}.

disperse more readily here, because they do not feel the restraining effect of a strong potential vorticity gradient.

d. Dependence of the solution on k_1^* and ϵ^*

Substituting into the integral stress balance (32), and using (18), it can be written (integrating, nondimensionalizing and rearranging)

$$\int_0^1 \bar{u}_3^* dy^* = \frac{2}{\pi^2} \frac{\delta_1}{\delta_3} \left(\frac{1}{\epsilon^*}\right)\left(\frac{u_S}{u_C}\right). \tag{33}$$

So, given the surface stress (and hence u_S), the transport of the lower layer is inversely proportional to ϵ^* and is independent of the K's.

The upper layer steady-state momentum equation can be written [integrating (19a) with respect to y and rearranging]

$$\frac{\partial \bar{q}_1^*}{\partial y^*} = \frac{1}{k_1^*}\left(\frac{u_S}{\pi\gamma u_C}\right)\frac{\sin\pi y^*}{Y^*}. \tag{34}$$

Our k_1^* then fixes the magnitude of $\partial \bar{q}_1^*/\partial y^*$ and hence [because $\partial \bar{q}_1^*/\partial y^*$ is dominated by $(\bar{u}_1^* - \bar{u}_3^*)/\delta_1$], the magnitude of the velocity difference between the two layers.

As k_1^* and ϵ^* are varied, the velocity profiles remain approximately equivalent barotropic. $\bar{u}_3^*$ is insensitive to the value of k_1^* and $(\bar{u}_1^* - \bar{u}_3^*)$ insensitive to the value of ϵ^*. If the bottom drag coefficient ϵ^* is held constant and the eddy diffusivity k_1^* increased, the velocity difference decreases—

the flow becomes more barotropic because the eddies are transferring momentum downward more efficiently. The lower layer potential vorticity becomes less negative and, by (17), the lower layer diffusivity larger.

5. A closure for the heat flux

So far it has only been necessary to make a closure hypothesis about the eddy flux of potential vorticity. It is necessary, however, to introduce additional hypotheses, if it is wanted to decompose the eddy potential vorticity flux into its component parts (e.g., to compute the vertical velocity and the energy exchanges between the mean and eddy fields).

Here a theory deriving from Green (1970) is formulated, in the context of the two-layer equations, and used to predict for the heat flux at the interface, and hence the layer relative vorticity fluxes.

The eddy flux of heat is related to the mean fields by the following non-isotropic diffusion equation (see Green, 1970).

$$\overline{v_2'(\psi_1' - \psi_3')} = -K_2 \frac{\partial}{\partial y} (\bar\psi_1 - \bar\psi_3)$$

$$- K_{vz} \frac{g'}{f_0} , \quad (35)$$

where K_2 and K_{vz} are transfer coefficients defined at the interface. For baroclinic disturbances, eddy heat transfer will take place not purely in the horizontal but along planes inclined at some angle. The second term in K_{vz}, involving correlations between eddy north-south velocities and vertical displacements, takes account of such baroclinic slope effects.

As before, a constraint is used to assist in the specification of the transfer coefficients.

a. A constraint on the layer vorticity flux

Integrating (10a) and (10b) across the channel, the layer eddy vorticity fluxes vanish to give

$$\frac{f_0^2}{g'} \int_0^L \overline{v_2'(\psi_1' - \psi_3')} dy$$

$$= -H_1 \int_0^L \overline{v_1'q_1'} dy = H_3 \int_0^L \overline{v_3'q_3'} dy. \quad (36)$$

Eq. (36) applies at all times, but in the particular case of the steady state, because of (30) it can be written as

$$\frac{f_0^2}{g'} \int_0^L \overline{v_2'(\psi_1' - \psi_3')} dy = \int_0^L \bar\tau_1 dy = \int_0^L \bar\tau_3 dy. \quad (37)$$

Eq. (37) suggests that, in the present two-layer formulation, it is instructive to view the interface

heat flux term as a pressure drag exerted by one layer on the other. This interpretation is clear once it is written in the form

$$\overline{f_0\psi_2' \frac{\partial h_I'}{\partial x}} \equiv \frac{f_0^2}{g'} \overline{v_2'(\psi_1' - \psi_3')}.$$

The term is a product of a pressure $f_0\psi_2'$ and an interface slope $(\partial h_I'/\partial x)$, and so is in the form of a drag. It is the mechanism by which the effect of the surface stress is transmitted down to the bottom. The pressure drag is an internal transfer of momentum in the vertical, just as the vorticity flux is an internal transfer of momentum in the horizontal (see Rhines and Holland, 1979).

b. Choice of K_2 and K_{vz}

Substituting for $\overline{v_2'(\psi_1' - \psi_3')}$ in (36), using (35), gives a relation analogous to (13), but this time between K_2 and K_{vz}

$$\int_0^L \left(K_2 \frac{\partial \bar h_I}{\partial y} - K_{vz}\right) dy = - \frac{H_1}{f_0} \int_0^L \overline{v_1'q_1'} dy \quad (38)$$

If (35) is to be used as the closure, it is important that the K_2 and K_{vz} chosen should satisfy this integral relation. Here K_2 and the meridional variation of K_{vz} are prescribed. The magnitude of K_{vz} is then adjusted until (38) is satisfied.

Following Green (1970), it is supposed the transfer coefficients are independent of the transferred quantity so long as it is closely conserved. Accordingly, K_2 (defined at the interface) is assumed to be a weighted average of K_1 and K_3, i.e.,

$$K_2 = k_2 Y(y) \quad (39a)$$

with

$$k_2 = \delta_3 k_1 + \delta_1 k_3. \quad (39b)$$

In the absence of any detailed knowledge of the form of K_{vz}, its meridional variation is taken to be the same as K_2:

$$K_{vz} = k_{vz} Y(y). \quad (40)$$

The magnitude k_{vz} is then adjusted so that (38) is satisfied.

Some interpretation of the relative magnitude of k_{vz} is possible if, as before, the curvature terms are neglected in the absolute vorticity gradient ($\bar\beta_1$, $\bar\beta_3 \approx \beta_0$). Then (38) may be written [using (15), (16), (17), (39) and (40)] in the simplified form

$$\frac{k_{vz}}{k_2} = \nu \overline{\frac{\partial \bar h_I}{\partial y}}^y , \quad (41)$$

where ν is a nondimensional number (a measure of the efficiency of conversion of available potential energy) given by

$$\nu = \frac{\gamma_1\gamma_3}{1 - \delta_1\gamma_1 + \delta_3\gamma_3} .$$

For unstable eastward flows, $\gamma_3 < 1$ and

$$0 < \nu < 1; \quad \frac{k_{vz}}{k_2} < \frac{\overline{\partial \bar{h}_I}^y}{\partial y}$$

and

$$k_{vz} > 0.$$

For unstable westward flows, $|\gamma_1| < 1$ and

$$0 < \nu < 1; \quad \left|\frac{k_{vz}}{k_2}\right| < \left|\frac{\overline{\partial \bar{h}_I}^y}{\partial y}\right|$$

and

$$k_{vz} < 0.$$

The ratio k_{vz}/k_2, given by (41), is therefore consistent with the necessary condition that, in order to release mean available potential energy, there must be a positive correlation between v' and z' in a positive shear, and a negative correlation in a negative shear. Further, on the average, typical particle paths should have a slope (measured by the ratio k_{vz}/k_2) less than the mean slope of the interface (ν should lie between 0 and 1).

It is worth emphasizing that the profiles of velocity and potential vorticity and the eddy flux of potential vorticity (Fig. 1) do not depend on any of these additional assumptions—they are independent of the relative contribution that the eddy wave drag and eddy vorticity flux makes to the eddy potential vorticity flux.

The interface eddy drag for the steady-state solution of Fig. 1 has been calculated using the above closure theory. The eddy layer relative vorticity fluxes can then be obtained from (10). The decomposition of the eddy potential vorticity flux into its component parts is shown in Fig. 2. Fig. 2a shows the upper layer momentum budget and Fig. 2b shows the lower layer momentum budget. The eddy drag makes up the major part of the potential vorticity flux in both layers, although in the upper layer the relative vorticity flux contributes significantly. The wind is a source of upper layer eastward momentum at all latitudes. Locally the wind stress is balanced mainly by the interfacial eddy drag, but the eddy vorticity flux is also important, concentrating the upper layer velocity. The eddy drag, which is a sink of eastward momentum in the upper layer, is a source for the lower layer. The bottom stress is the ultimate momentum sink, locally balancing the interfacial stress. The lower layer eddy vorticity flux only makes a small contribution to the budget.

6. Comparison with an eddy-resolving channel simulation

Of the MHC Circumpolar Current simulations, the channel flow (CH in their notation) corresponds most closely to the parameterized model. It has a flat bottom, is driven by a steady wind stress and there is minimal explicit diffusion. For comparison,
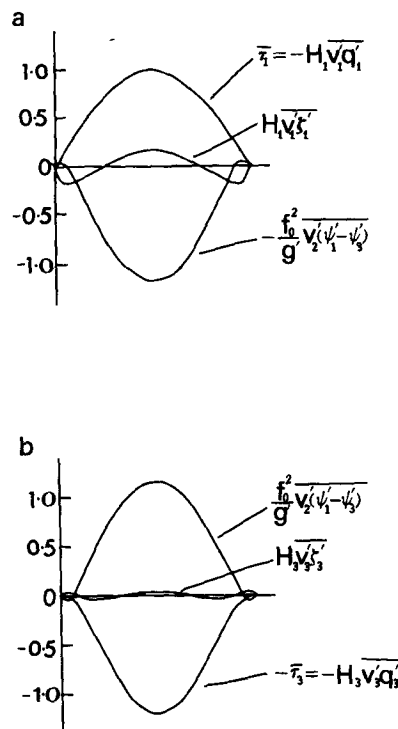

FIG. 2. Terms in the layer momentum equations for the steady-state solution $k_1^* = 0.18$. (a) Upper layer momentum budget $\bar{\tau}_1 + H_1\overline{v_1'\xi_1'} - (f_0^2/g')\overline{v_2'(\psi_1' - \psi_3')} = 0$; (b) lower layer momentum budget $-\bar{\tau}_3 + H_3\overline{v_3'\xi_3'} + (f_0^2/g')\overline{v_2'(\psi_1' - \psi_3')} = 0$. Units are in 10^{-4} m^2 s^{-2}.

the time and zonally averaged zonal velocity and eddy statistics of the CH simulation are shown in Fig. 3. Fig. 3a should be compared with Fig. 1a, Fig. 3b with Fig. 1d, and Fig. 3c with Fig. 2a.

It is not surprising that the two models develop mean flows and eddy fluxes of comparable magnitude. The bottom-friction coefficient ϵ^* [which, from (33), determines the magnitude of the lower layer flow] is the same in both, and k_1^* [which, from (34), determines the velocity difference between the layers] was chosen to correspond to the upper layer diffusivity estimated from CH. Further, the eddy fluxes were constrained to satisfy the necessary integral balances.

The parameterized model fails to reproduce the sharper meridional profiles of the explicit model. Such details depend on the particular form of $Y(y)$ which, at best, can only be specified crudely. The eddy wave drag is also less peaked in midchannel (and hence, locally, the eddy vorticity flux is underestimated). The reasons are less clear because of the additional closure assumptions made in its calculation: the transfer coefficients for heat and potential vorticity are assumed to be the same, and it is necessary to introduce an extra coefficient to take account of the slantwise nature of this aspect of the instability.
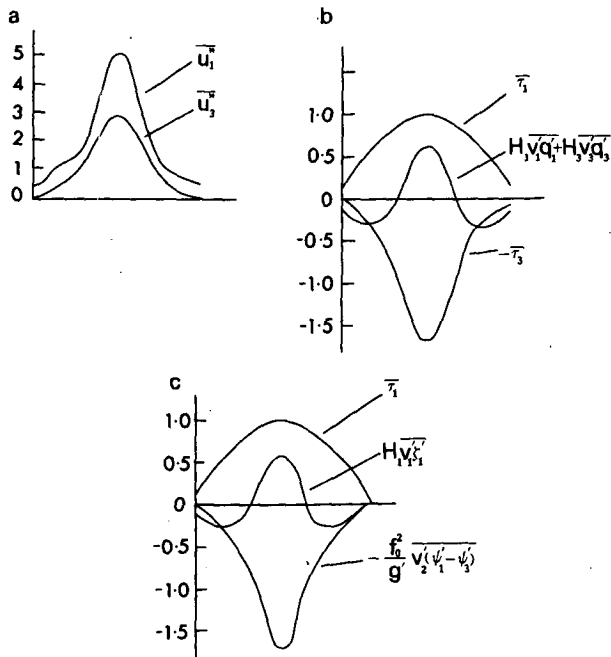
FIG. 3. Time and zonally averaged meridional profiles of the McWilliams *et al.* (1978) CH simulation: (a) nondimensionalized zonal velocity; (b) depth-integrated momentum budget in units of 10^{-4} m^2 s^{-2}; and (c) upper layer momentum budget in units of 10^{-4} m^2 s^{-2}.

Despite these differences, the general agreement is good. The interior fluxes, attributed to a mesoscale eddy field and incorporated here parametrically, show the same structure and are playing the same dynamical role as the fluxes achieved by the resolved eddies of the MHC simulations.

7. Westward flow

The instability properties of westward flows are of interest in the ocean because westward flows are more susceptible to baroclinic instability than eastward flows. For example, in the Holland (1978) two-layer model, because the upper layer is thinner than the lower layer, it is the return flow recirculation region of the inertial gyres which are often favored as eddy generation sites. The flow becomes unstable due to the presence of large negative shears. In this section, a westward channel flow regime is studied using the parameterized model.

A negatively sheared flow can easily be produced by applying a surface stress directed toward the west

$$\bar{\tau}_1 = -\tau_0 \sin\left(\frac{\pi y}{L}\right) .$$

Fig. 4 shows the steady-state solution for the case $k_1^* = 1.8$. Given (29), the k_1^* corresponds to a k_1 of
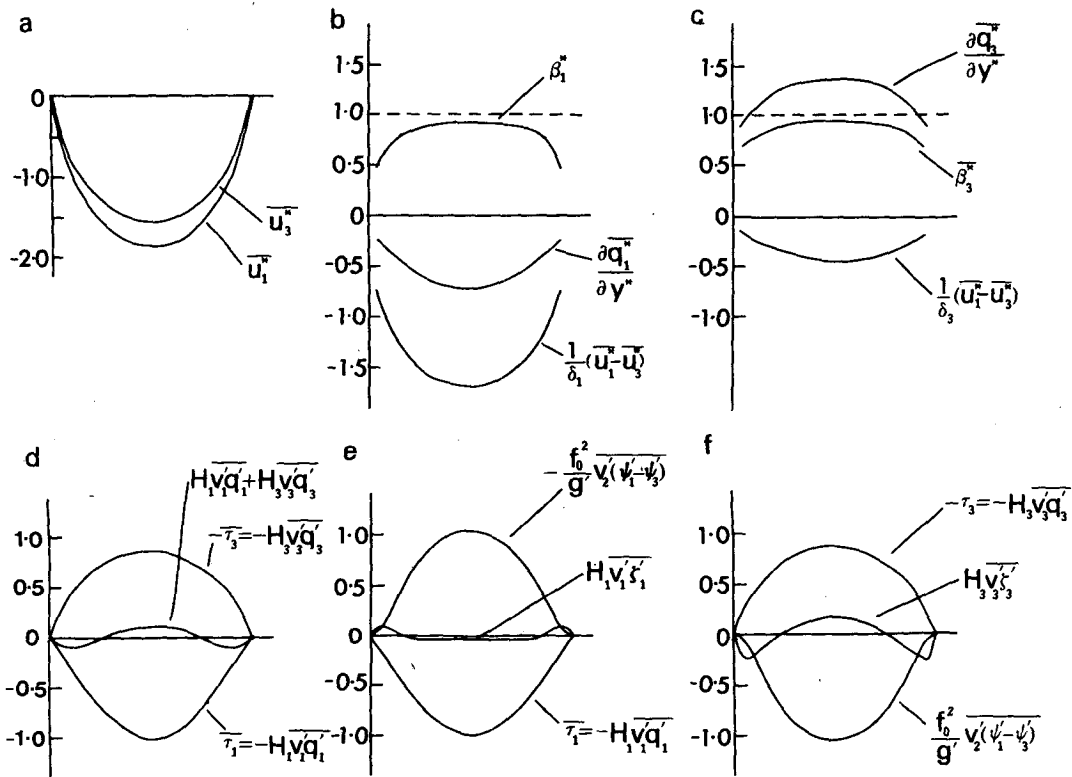

FIG. 4. Meridional profiles for the steady-state, negatively sheared solution, $k_1^* = 1.8$: (a) nondimensionalized zonal velocity; (b) nondimensionalized upper layer potential vorticity gradient; (c) nondimensionalized lower layer potential vorticity gradient; (d) depth-integrated momentum budget in units of 10^{-4} m^2 s^{-2}; (e) upper layer momentum budget in units of 10^{-4} m^2 s^{-2}; and (f) lower layer momentum budget in units of 10^{-4} m^2 s^{-2}.

10^4 m^2 s^{-1}, and is chosen as a realistic value for an upper ocean eddy diffusivity in the near field of the Gulf Stream.

The zonal velocity, Fig. 4a, is negatively sheared and to the west. The potential vorticity distribution, Figs. 4b and 4c, is very different from the eastward flow case. The upper layer potential vorticity gradient is now negative, and the lower layer gradient positive. The absolute vorticity gradient and velocity shear both contribute importantly. The upper layer gradient is reversed due to the presence of negative shear.

The terms in the vertically integrated, upper layer and lower layer steady-state momentum equations are shown in Figs. 4d, 4e and 4f, respectively. The wind is the source, and the bottom stress the sink of westward momentum at all latitudes. The eddy wave drag acts as the source of lower layer westward momentum. Momentum is redistributed in the horizontal by the relative vorticity flux, mainly in the lower layer. The eddy field concentrates eastward momentum in midchannel. Since the mean flow is already toward the west, the effect of the eddies is to retard the mean flow here. The meridional pattern of eddy relative vorticity flux indicates a net transfer from the mean to the eddy kinetic energy. The sharpening of the unstable jets due to upgradient momentum transfer is not occurring here. The usually accepted transfer from eddy to mean kinetic energy is a characteristic of positively sheared (westerly) flows. Baroclinic eddies developing on negatively sheared (easterly) flows can be expected to transfer kinetic energy in the opposite direction. This is a point made by Held (1975). Some support for the sign of the kinetic energy transfer occurring in unstable negatively sheared flow is provided by the Holland (1978) gyre simulations. Here the return flow of the inertial gyre becomes baroclinically unstable, and the effect of the eddies is to retard the mean flow as suggested by our transfer theory.

In the steady state the ratio of the transfer coefficients is $k_3/k_1 = 0.11$ giving a lower layer diffusivity of $k_3 = 1.1 \times 10^3$ m^2 s^{-1} for a k_1 of 10^4 m^2 s^{-1}. In contrast to eastward flows, the K's are biased to the surface.

If the proposed parameterization scheme is a true representation of the interaction between mean flow and eddies, then Fig. 4 should give a reasonable picture of the mean and eddy fields to be expected in a baroclinically unstable negatively sheared zonal flow. The details await verification from an eddy-resolving channel model.

8. Welander's potential vorticity transfer theory

Welander (1973) derived an eddy transfer theory for an ocean gyre which proposed that geostrophic eddies could generate a net meridional flux of vorticity due to the β-effect, and so enhance

the Gulf Stream transport obtained from linear Sverdrup theory. Here the two-layer equivalent of Welander's continuous formulation is derived, to put it in the context of the present work.

Substituting in (11) for the eddy fluxes of potential vorticity, using (9), gives

$$H_1 \overline{v_1' \xi_1'} + H_3 \overline{v_3' \xi_3'}$$

$$= -H_1 K_1 \frac{\partial \bar{q}_1}{\partial y} - H_3 K_3 \frac{\partial \bar{q}_3}{\partial y}. \quad (42)$$

Welander's formulation can be regarded as an approximated form of (42). He made the following simplifications:

1) The transfer coefficients were not allowed to vary in space:

$$K_1 = K_3 = K, \quad \text{a constant.}$$

Then (42) reduces to

$$H_1 \overline{v_1' \xi_1'} + H_3 \overline{v_3' \xi_3'} = -K(H_1 \bar{\beta}_1 + H_3 \bar{\beta}_3). \quad (43)$$

The constant K condition is equivalent to approximating the potential vorticity gradient by the absolute vorticity gradient.

2) The relative vorticity gradient was neglected in the absolute vorticity gradient:

$$\bar{\beta}_1 = \bar{\beta}_3 = \beta_0.$$

Then (43) reduces to

$$H_1 \overline{v_1' \xi_1'} + H_3 \overline{v_3' \xi_3'} = -KH\beta_0. \quad (44)$$

Eq. (44) is of the form adopted by Welander and approximates the potential vorticity gradient by the planetary vorticity gradient.

The appropriateness of the approximated forms (43) and (44) to channel flow can be ascertained by noting that the integrated vorticity flux must vanish, giving

$$K \int_0^L H_1 \bar{\beta}_1 + H_3 \bar{\beta}_3 \, dy = 0, \quad (45)$$

$$K \int_0^L \beta_0 \, dy = 0. \quad (46)$$

From (45), for instability ($K > 0$) the absolute vorticity gradient must change sign somewhere in the flow: the relative vorticity gradient must become large enough to balance β, allowing a barotropic instability. If the relative vorticity gradient is negligible, then from (46), the only possibility is stable flow ($K = 0$) and in this case vorticity is not transferred.

Applying (44) to channel flow would give unphysical results since it predicts a southwards vorticity flux everywhere, and so produces a force which is everywhere toward the west. As Welander (1973) points out:

". . . the predicted westward friction force, $-k\beta$, can be physically realized only in the presence of some meridional wall. An ocean covering the earth entirely would, due to this term, be accelerated westward everywhere, thereby contradicting the angular momentum conservation principle."

Such consequences of vorticity mixing led Thomson and Stewart (1977) to question the validity of Welander's (1973) application of vorticity transfer theory and, later, in Stewart and Thomson (1977) the validity of vorticity transfer itself was challenged on fundamental grounds. They suggest that, despite vorticity being a more conservative and hence a more transferable quantity than momentum, momentum transfer theory should be favoured over vorticity transfer theory because the latter can lead to non-conservation of overall momentum. However, vorticity transfer theory is not fundamentally incorrect because for arbitrary forms of the transfer coefficient it can violate momentum conservation. At infinitesimal amplitude the theory is an exact theory (because the K's are exactly known) and so it satisfies all the necessary integral constraints. Furthermore, in fully turbulent flow, the K's can always be chosen in order that a momentum constraint be satisfied. Indeed, the existence of a momentum constraint in our channel model is a distinct practical advantage for it can be exploited to give information about the K's. In the closed ocean-basin model considered by Welander (1973), though, because the meridional walls may resupply momentum and so support a net meridional vorticity flux, there is no angular momentum constraint. In this case no extra information about the form of the K's can be gained from a consideration of the angular momentum.

The westward flow that can occur as a consequence of the mixing of potential vorticity if $\partial \bar{q}/\partial y$ is dominated by β_0, is illustrated in the laboratory experiment of Whitehead (1975) which is further discussed in Rhines (1977). On a homogeneous β-plane eddies are generated locally in the previously still fluid by a means that does not supply angular momentum. Away from the source region westward flow develops, as one would expect if the eddies were mixing potential vorticity. In the region of the forcing, however, a compensatory eastward flow develops. Here there is upgradient flux and the diffusive transfer theory is invalid.

In our channel model we require the eddies to be generated by a fluid instability. In this case a Rayleigh criterion must be satisfied. Then the source region for the eddies is a dynamically unstable one, and the northward vorticity flux required to conserve overall zonal momentum may still be achieved by downgradient transfer, for the mean potential vorticity gradient has now changed sign to become

negative. Here the fluid is accelerated to the east. In the quieter regions, to the north and south of the unstable jet, the potential vorticity gradient is positive (dominated by β) and, as in the Welander (1973) closure and the Whitehead (1975) experiment, there is southward vorticity flux here, and the fluid is accelerated to the west.

9. Future developments

The present work should be regarded as a preliminary investigation before tackling flow in the zonally blocked geometry more typical of the ocean. It would be interesting, for example, to see if it is possible to reproduce the lower layer, tight gyres of the Holland (1978) simulations using a parameterized model. This is not expected to be a straightforward task, for here the integral constraints on the eddy motion are less clear and the appropriateness of a diffusive parameterization for potential vorticity doubtful.

REFERENCES

Gill, A. E., 1971: Ocean models. *Phil. Trans. Roy. Soc. London,* A27, 391–414.

Green, J. S. A., 1970: Transfer properties of the large-scale eddies and the general circulation of the atmosphere. *Quart. J. Roy. Meteor. Soc.,* 96, 157–185.

Harrison, D. E., 1978: On the diffusion parameterization of mesoscale eddy effects from a numerical ocean experiments. *J. Phys. Oceanogr.* 8, 913–918.

Held, I. M., 1975: Momentum transport by quasi-geostrophic eddies. *J. Atmos. Sci.,* 32, 1494–1497.

Holland, W. R., 1978: The role of mesoscale eddies in the general circulation—numerical experiments using a wind-driven quasi-geostrophic model. *J. Phys. Oceanogr.,* 8, 363–392.

——, and L. B. Lin, 1975a: On the origin of mesoscale eddies and their contribution to the general circulation of the ocean. I. A preliminary numerical experiment. *J. Phys. Oceanogr.,* 5, 642–657.

——, and L. B. Lin, 1975b: On the origin of mesoscale eddies and their contribution to the general circulation of the ocean. II. A parameter study. *J. Phys. Oceanogr.,* 5, 658–669.

——, and P. B. Rhines, 1980: An example of eddy-induced ocean circulation. *J. Phys. Oceanogr.,* 10, 1010–1031.

Hoskins, B. J., and A. J. Simmons, 1978: The life cycle of some non-linear baroclinic waves. *J. Atmos. Sci.,* 35, 414–432.

McWilliams, J. C., 1977: A note on a consistent quasi-geostrophic model in a multiply-connected domain. *Dyn. Atmos. Oceans.,* 7, 427–441.

——, W. R. Holland, and J. H. S. Chow, 1978: A description of numerical Antarctic Circumpolar Currents. *Dyn. Atmos. Oceans,* 2, 213–291.

Munk, W. H., 1950: On the wind-driven circulation. *J. Meteor.,* 7, 79–93.

Pedlosky, J., 1964: The stability of currents in the atmosphere and the ocean. *J. Atmos. Sci.,* 21, 201–219.

Rhines, P. B., 1977: The dynamics of unsteady currents. *The Sea*, Vol. 6, 189–318.

——, and W. R. Holland, 1979: A theoretical discussion of eddy-driven mean flows. *Dyn. Atmos. Oceans.*, **3**, 289–325.

Robinson, A. R., D. E. Harrison, Y. Mintz and A. J. Semtner, 1977: Eddies and the general circulation of an idealized oceanic gyre: A wind and thermally driven primitive equation numerical experiment. *J. Phys. Oceanogr.*, **7**, 182–207.

Schmitz, W. J., 1977: On the deep general circulation in the western North Atlantic. *J. Mar. Res.*, **35**, 21–28.

Sela, J., and A. Wiin-Nielson, 1971: Simulation of the atmospheric energy cycle. *Mon. Wea. Rev.*, **99**, 460–468.

Semtner, A. J., and Y. Mintz, 1977: Numerical simulation of the Gulf Stream and mid-ocean eddies. *J. Phys. Oceanogr.*, **7**, 208–230.

Stewart, R. W., and Thomson, R. E., 1977: Re-examination of vorticity transfer theory. *Proc. Roy. Soc. London*, **A354**, 1–8.

Simmons, W., and the MODE Group, 1977: The mid-ocean dynamics experiment. *Deep-Sea Res.*, **25**, 859–910.

Thomson, R. E., and R. W. Stewart, 1977: The balance and redistribution of potential vorticity within the ocean. *Dyn. Atmos. Oceans*, **1**, 299–321.

Veronis, G., 1966: Wind-driven ocean circulation: Part II. Numerical solutions of the non-linear problem. *Deep-Sea Res.*, **13**, 31–55.

Webster, F., 1961: The effect of meanders on the kinetic energy balances of the Gulf Stream. *Tellus*, **13**, 392–401.

Welander, P., 1973: Lateral friction in the ocean as an effect of potential vorticity mixing. *Geophys. Fluid Dyn.*, **5**, 101–120.

White, A. A., 1977: The surface flow in a statistical climate model—a test of a parameterization of large-scale momentum fluxes. *Quart. J. Roy. Meteor. Soc.*, **103**, 93–119.

——, and J. S. A. Green, 1980a: Transfer coefficient eddy flux parameterizations in a simple model of the zonal average atmospheric circulation. To be submitted to the *Quart. J. Roy. Meteor. Soc.*

——, and ——, 1980b: A non-linear atmospheric long wave model incorporating parameterizations of transient baroclinic eddies. To be submitted to *Quart. J. Roy. Meteor. Soc.*

Whitehead, J. A. Jr., 1975: Mean-flow driven by circulation on a β-plane. *Tellus*, **27**, 358–364.